Design of Practical In-Service Fault-Isolating System for Optical Passive Double Star Networks

Yamamoto, Fumihiko
Department of Computer Science and Communication Engineering, Graduate School of Information Science and Electrical Engineering, Kyushu University : Graduate Student

Yasumoto, Kiyotoshi
Department of Computer Science and Communication Engineering, Faculty of Information Science and Electrical Engineering, Kyushu University

https://doi.org/10.15017/1515732

出版情報：九州大学大学院システム情報科学紀要. 6 (2), pp.169-178, 2001-09-26. 九州大学大学院システム情報科学研究院
バージョン：
権利関係：

九州大学大学院
システム情報科学紀要
第6巻　第2号　平成13年9月

Research Reports on Information Science and
Electrical Engineering of Kyushu University
Vol.6, No.2, September 2001

Design of Practical In-Service Fault-Isolating System for Optical Passive Double Star Networks

Fumihiko YAMAMOTO* and Kiyotoshi YASUMOTO**

(Received June 15, 2001)

Abstract: This paper describes a practical technique and system design for isolating faults in an actually working optical fiber or optical transmission equipment in passive double star (PDS) networks which have optical splitters located outside a central office. The fault-isolating system contributes to the reduction of the restoration time for optical PDS networks since the fault isolation enables maintenance engineers to know what to do first when repairing the networks. An optical time domain reflectometer (OTDR) with a high spatial resolution of 1 m and short wavelength pass filters (SWPF) for 1.6-μm region are key devices in the system. The reflection from the SWPF is observed by using the OTDR in the fault isolation. Since the OTDR owns the high resolvability, the OTDR trace can show the level and position of the peak due to the reflection from each SWPF in an optical PDS networks. In this paper, the practical requirements of the key devices are made clear for implementation of the fault isolation. Moreover, we show those proprieties resulting from employing our fault isolation system in a field experiment on new multimedia info-communication services in Japan.

Keywords: Optical time domain reflectometer, Short wavelength pass filter, In-service testing, Fault isolation, Passive double star networks

1. Introduction

In recent years, optical access networks with a passive double star (PDS) topology have been extensively investigated throughout the world[1)-8)]. This is because it is very important to reduce the system cost for the optical access networks since the charge to the customer depends heavily on the system cost. The optical PDS architecture allows one optical line terminal (OLT) installed in a central office to be shared among many optical network units (ONU) on customers' premises. This feature can provide a significant advantage in that the cost can be spread among many subscribers, and the use of the optical PDS topology reduces the system cost.

If an operator can remotely specify a network fault in either optical fibers or transmission equipment, it leads to quick restoration of the network. This is because this ability to specify, which is called 'fault isolation', enables maintenance engineers to know what to do first when repairing the networks. Such a testing has already been proposed for operating single star (SS) networks[9)-11)]. In this technique, a specific wavelength of 1.55 μm, being different from a signal wavelength of 1.31 μm, is assigned to measure working fibers. A short wavelength pass filter (SWPF) that reflects only the 1.55-μm measurement light is installed in front of an ONU. Faults are isolated by measuring Fresnel reflection from the SWPF with an optical time domain reflectometer (OTDR) installed in a central office.

When the fault isolation technique for the SS network is applied to an optical PDS network in which an optical splitter is located outside the central office, optical pulses from the OTDR are distributed to all branched optical fibers via the optical splitter. Since all the Fresnel reflections from SWPFs enter the OTDR via the splitter, they are superimposed in one OTDR trace. In the PDS networks, the spatial resolution of the OTDR becomes more important than that in the SS networks. The spatial resolution Δz corresponds to a half of the OTDR pulse length on the fiber, and is given by

$$\Delta z = \nu_{gr} \cdot W_p / 2 \qquad (1)$$

where ν_{gr} is the group velocity, and W_p is the pulse width of the OTDR. If the spatial resolution is more than the deference between the lengths of the branched fibers, it is very difficult to measure the reflected peak level and the distance from the central office to each SWPF by analyzing the trace. One way to solve the problem is to assign

* Department of Computer Science and Communication Engineering, Graduate Student
** Department of Computer Science and Communication Engineering

multi-wavelengths for testing and to add the wavelength-dependent return loss to the SWPF[12]. However, it makes a fault-isolating system complex.

This paper describes a practical design for implementing in-service fault isolating at a single wavelength. The system has two key devices. One is an OTDR with high spatial-resolution that is a consequence of narrowing its pulse width and widening its receiver bandwidth. The operating wavelength is designed to be in a 1.6-μm band because wavelengths of 1.31 μm and 1.55 μm are assigned to bi-directional communication[2] and broadcasting[4] services, respectively. The other key device is a newly designed SWPF that allows 1.31-μm and 1.55-μm signal lights to pass but reflects the 1.6-μm band measurement light. Section 2 discusses the system configuration for isolating a fault in a working optical PDS network with an outside splitter. In Sec. 3, we develop a design procedure for the two key devices mentioned above. This section also discusses the practical goals that would allow these key devices to be used for fault isolation. Section 4 presents experimental results on the performance of the designed system. Finally, Sec. 5 demonstrates the field trial experiments using a proposed in-service fault-isolating system.

2. System Configuration for Fault Isolation

2.1 Optical PDS System

Figure 1 shows the configuration of an optical PDS system incorporating a wavelength division multiplexing (WDM) technique[13]. The transmission line, which is less than 7-km long, is composed of a non-branched common optical fiber, an optical splitter and branched optical fibers. The common fiber is split into a maximum of 16 optical fibers with an optical splitter. The splitter is located in the field since the use of a long common fiber makes the constructed fiber cost low. An OLT is installed in a central office, and is connected with the line through a wavelength insensitive coupler (WINC). ONUs installed on customer premises are joined to the other end of the line. A signal with a wavelength of 1.31 μm is used for bi-directional communication services, such as the integrated services digital network (ISDN), by employing a synchronous transfer mode (STM) technique. In addition, a signal with a wavelength of 1.55 μm is used for video distribution services with a subcarrier multiplexing (SCM) technique. After signals of STM and SCM from the OLT are divided

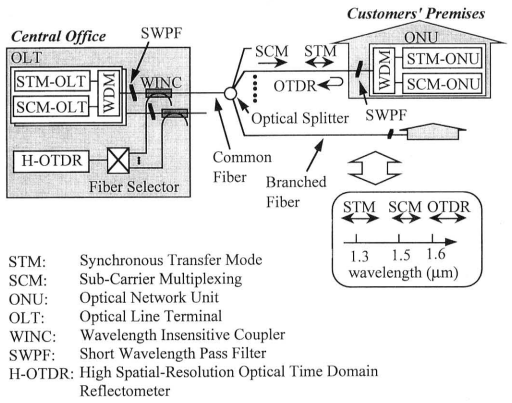

Fig.1 Schematic illustration of a fault-isolating system in a working optical passive double star (PDS) network. The feature of the network is that the optical splitter is positioned outside the central office.

with a WDM filter equipped in the ONU, each signal is received at each terminal.

2.2 Fault-Isolating System

To achieve remote fault isolation in an optical PDS network, a high spatial-resolution OTDR (H-OTDR) operating in a 1.6-μm band is installed in a central office, as shown in **Fig.1**. An SWPF, which is an optical filter embedded in a single-fiber-coupling (SC) connector, is positioned at the input port of each ONU. The SWPF allows only 1.31-μm and 1.55-μm signal lights to pass and to reflect the measurement light in the 1.6-μm band. The 1.6-μm band measurement is adopted because, being a longer wavelength, it is more sensitive to fiber bending losses than the 1.31-μm and 1.55-μm bands. This extra sensitivity allows anomalies occurred in an optical fiber to be identified before it breaks down.

When carrying out fault isolation, a test fiber is connected to the H-OTDR with a fiber selector. An optical pulse from the H-OTDR propagates through the transmission line via the fiber selector and the WINC, and is reflected at each SWPF. The back-reflected pulses are superimposed in one H-OTDR trace via the optical splitter. The trace can show the level and position of peak due to the reflection from each SWPF because of high resolvability of the H-OTDR. The H-OTDR trace is stored at every time of measurements. Then, transmission line faults can be distinguished from ONU faults by comparing a new trace with the stored trace. By identifying any missing peaks or new reflections, we can isolate a fault in one particular fiber from

among all the fibers in an optical PDS network.

3. Design of Key Devices for Fault Isolation

3.1 1.6-μm Band SWPF Embedded in SC-Connector

It is very important to estimate the required transmission loss of an SWPF for the measurement wavelength since H-OTDR light could affect the signal quality of STM and SCM. In this subsection, we assume that the required transmission loss of the SWPF can be estimated by considering only the video quality of an SCM signal with a wavelength of 1.55 μm under in-service testing. The H-OTDR light hardly propagate to the STM port being separated with a WDM filter installed in an ONU, because the wavelength of STM signals is much shorter than that of the H-OTDR light.

In front of the ONU, the H-OTDR light power must become weak enough to maintain the SCM signal quality in the presence of H-OTDR light. In other words, the weak H-OTDR light is allowed to enter the ONU. Since subcarrier frequencies are usually in high frequency region (*e.g.*, above 90 MHz[13]), the allowable received power for the H-OTDR light at the ONU depends on the pulse spectrum of the H-OTDR light. The allowable received optical peak power P_{allow} of the OTDR light is given by[14]

$$P_{\text{allow}}^2 = (\Delta_{\text{CNR}} - 1) \cdot \frac{S_{\text{subcarrier}}}{N_{\text{OTDR}}} \cdot \text{CNR}_0^{-1} \tag{2}$$

where $S_{\text{subcarrier}}$ corresponds to the average received subcarrier signal power at the ONU, N_{OTDR} corresponds to the total noise power induced by the OTDR light at the ONU, CNR_0 is the value of the carrier-to-noise ratio (CNR) when the OTDR light is excluded, and the tolerance Δ_{CNR} for the CNR decrease caused by the OTDR light is defined by

$$\Delta_{\text{CNR}} = \text{CNR}_0 / \text{CNR}. \tag{3}$$

$S_{\text{subcarrier}}$ is given by

$$S_{\text{subcarrier}} = \frac{1}{2}(\text{OMI} \cdot P_{ls})^2 \tag{4}$$

where OMI is the optical intensity modulation index per channel and P_{ls} is the average received signal light power at the ONU. The spectral components of the pulse fallen in one channel are significant noise in N_{OTDR}. This noise is called pulse-induced noise in this paper. Since the pulse-induced noise is extremely larger than the other types of noise caused by the OTDR light, such as the intensity fluctuation noise of the light source and shot noise, N_{OTDR} is assumed to be given by only the pulse-induced noise for simple discussion. N_{OTDR} in one channel with a subcarrier frequency of f_c and a bandwidth of B_{signal} is given by[14]

$$N_{\text{OTDR}} = \frac{1}{2}(\max \cdot [|n_{\text{pulse}}(t)|])^2 \tag{5}$$

and

$$n_{\text{pulse}}(t) = \sum_{n=n_1}^{n_2} 2 \cdot \left[f_0 W_p \cdot \frac{\sin(\pi n f_0 W_p)}{\pi n f_0 W_p} \right] \cdot \cos(2\pi n f_0 t) \tag{6}$$

with

$$\begin{aligned} n_1 &= f_c / f_0 + \varepsilon_1 \\ n_2 &= (f_c + B_{\text{signal}}) / f_0 + \varepsilon_2, \ |\varepsilon_{1,2}| < 1/2 \end{aligned} \tag{7}$$

where $n_{\text{pulse}}(t)$ is the temporal response function of the pulse train from a bandpass filter with one subcarrier frequency band, max·[] denotes the maximum value in the brackets, f_0 is the inverse of the OTDR pulse repetition cycle, and W_p is the pulse width. The integer values of n_1 and n_2 define the frequencies $n_1 f_0$ and $n_2 f_0$ which are the closest to the transmittable minimum and maximum frequencies of one subcarrier band, respectively.

Figure 2 shows the allowable received OTDR light power estimated from Eqs. (2) to (7) as a function of the OTDR pulse width W_p when Δ_{CNR} = 0.2dB. In this calculation, the SCM system parameters such as CNR_0 = 43dB, OMI = 0.045, P_{ls} = −7.7dBm, f_c =91.25MHz, and B_{signal} =4.2MHz were used in accordance with the SCM specifications[13]. With an increase in the pulse width, the allowable received power becomes almost independent of the pulse width. This is because many lobes in the spectrum of a wider pulse have fallen into one channel and hence the pulse-induced noise is not much affected by varying the pulse width. When the pulse width becomes less than $1/B_{\text{signal}}$, the allowable power becomes sensitive with a decrease in the pulse width, since the lobe width is wider than B_{signal}. Equation (1) shows that we must make the pulse width narrower to enhance the spatial resolution of the OTDR. When narrowing the pulse width from 1 μs to 10ns, the allowable peak power decreases by 3dB in the worst case. It can be seen that the transmission loss of the SWPF for the measurement wavelength

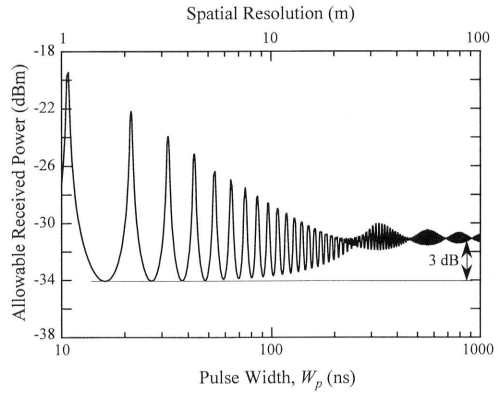

Fig.2 Dependence of the allowable received peak power for the OTDR light on pulse width at f_c = 91.25MHz. The spatial resolution is calculated from Eq. (1) with $\nu_{gr} = 2.0 \cdot 10^8$ m/s.

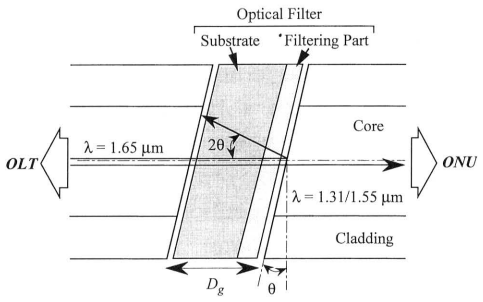

Fig.3 Configuration of an SWPF in which an optical interference filter is embedded in an SC connector.

must be more than 34dB if the peak power of the OTDR light with a pulse width of 10ns is 0dBm in front of the SWPF.

Figure 3 shows the configuration of an SWPF in which an optical interference filter is embedded in an SC connector. When the light is re-injected into the fiber with coupling efficiency η_c by reflection from the filter, the return loss R_{SWPF} is related to the filter inclination angle θ with respect to the fiber axis and the width D_g of the groove which is along the fiber axis as[15]

$$R_{SWPF} = [(1 - 1/L_{filter}) \cdot \eta_c(\theta, D_g)]^{-1} \tag{8}$$

with

$$\eta_c = \kappa \cdot \exp\left[-\kappa \left\{ \frac{(2D_g\theta)^2}{2}\left(\frac{1}{w_0^2} - \frac{1}{w_1^2}\right) + (2n_r\pi\theta)^2 \frac{(w_0^2 + w_1^2)}{2\lambda^2} \right\}\right] \tag{9}$$

$$\kappa = \frac{4w_0^2 w_1^2}{(w_0^2 + w_1^2)^2 + (\lambda^2 D_g^2 / n_r^2 \pi^2)} \tag{10}$$

and

$$w_1^2 = w_0^2\left[1 + \frac{(\lambda D_g)^2}{(n_r \pi w_0^2)^2}\right] \tag{11}$$

where L_{filter} is the transmission loss of the filter, W_0 is the mode field radius of the fiber in front of the filter, λ is the wavelength of the propagating light, and n_r is the refractive index difference between the filtering part and the optical fiber. Equation (8) shows that the return loss of the SWPF depends on the filter inclination angle and the groove width. The relations between the inclination angle and the groove width to realize several return loss values for the 1.65-μm wavelength are plotted in **Fig.4** by dotted curves, where w_0 = 6.3 μm, n_r = 1.45, and the filter transmission loss is 34dB. The solid curve shows the similar result for the signal wavelength of 1.55 μm when w_0 = 6.0 μm, n_r = 1.45, and the filter transmission loss is 0.15dB. For the system design, we must take account of the return losses for the wavelengths of both the OTDR and SCM lights, because the dynamic range of an H-OTDR depends on the return loss of the SWPF in the 1.6-μm band. The return loss for the SCM signal wavelength of 1.55 μm is also very important in terms of maintaining the signal quality because it is very sensitive to multiple connector reflections[16]. In the calculation, the return loss for the 1.55-μm wavelength was assumed to be more than 35dB. This value corresponds to the return loss of a conventional mechanically transferable (MT) connector whose structure is based on the plastic molded multifiber connector[17]. An interesting feature of **Fig.4** is that the return loss at the 1.65-μm wavelength must be more than 20dB for the return loss at the 1.55-μm wavelength to be more than 35dB.

When θ = 0 and $w_1 = w_0$, the transmission loss of the SWPF for the signal wavelength of 1.55 μm is evaluated from Eqs. (8), (9) and (10). If the groove widths are 30 μm and 100 μm, for example, the transmission losses for the 1.55-μm wavelength including the filter transmission loss of 0.15dB are more than 0.25dB and 1dB, respectively. The result implies that a narrower groove width is preferable to reduce the signal transmission loss of the SWPF. However, the groove width of more than 30 μm is requested for the optical filter to be fixed in the grooved glass substrate by adhesive[18]. It can be seen in **Fig.4** that the suitable inclination angle θ of the filter is around 3.5 degrees at D_g = 30 μm for obtaining the return

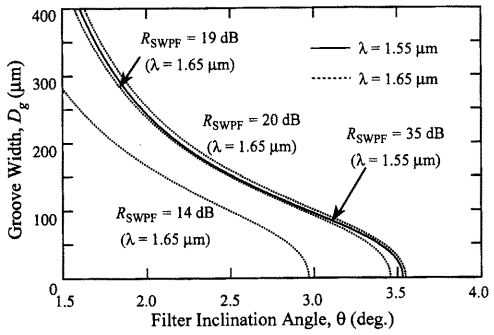

Fig.4 Relationship between the filter inclination angle and the width of the groove in which the optical interference filter is inserted for several return losses.

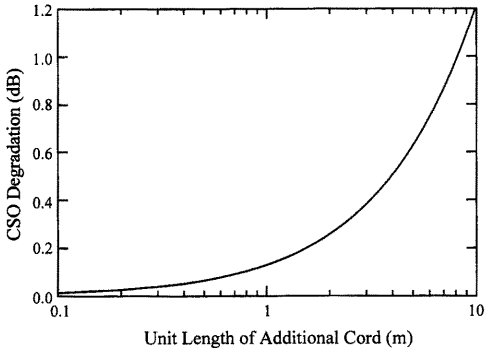

Fig.5 Dependence of CSO degradation on the unit length of the additional fiber cord. There are 16 branched fibers in one optical splitter. The difference ΔL_{fiber} between the original transmission fiber length and the compensating length of the DCF is 1km.

loss of 20dB for the 1.65-μm wavelength.

3.2 1.6-μm Band H-OTDR

It is not so easy to isolate the observed reflection from each SWPF in an H-OTDR trace even when the spatial resolution becomes higher. This is because there is still a slight possibility that the difference between the branched optical fiber lengths in one optical splitter is less than the spatial resolution of the H-OTDR. This problem can be resolved by incorporating fiber cords for adjusting the branched fiber lengths. The cords are used to make the difference longer than the spatial resolution. However, the signal quality may be degraded in the presence of the cords. The chromatic dispersion of the fiber affects the quality of the distortion of the SCM signal. In fact, a dispersion compensating fiber (DCF) is used to satisfy the required condition for the distortion in an optical PDS system[13]. Since the composite second-order (CSO) for the distortion is inversely proportional to the square of the fiber length[19], the degradation for CSO due to additional cords, Δ_{CSO}, is given by

$$\Delta_{CSO} = [\Delta L_{fiber} / (\Delta L_{fiber} + L_{add})]^{-2} \quad (12)$$

where ΔL_{fiber} is the difference between the original transmission fiber length and the compensating fiber length of a DCF, and L_{add} is the additional cord length. Here the dispersion in the transmission fiber and the optical cord were assumed to be same. Equation (12) shows that a longer cord degrades the CSO. When all the branched fiber lengths are same in the worst case, L_{add} to minimize the CSO degradation is given by

$$L_{add} = L_{cord} \cdot (NB_s - 1) \quad (13)$$

where L_{cord} is one unit of additional cord length, and NB_s is the maximum number of branches in one splitter. By adding the fiber cords, the difference between the branch lengths is relaxed to L_{cord} even for the worst case. In other words, the spatial resolution of the H-OTDR must be less than the unit cord length. **Figure 5** shows the theoretical result of the CSO degradation obtained from Eqs. (12) and (13) at ΔL_{fiber} = 1km and NB_s = 16. When the CSO decrease of 0.2dB is allowed, for example, the resolution must be less than 1.6m. This conclusion is a consequence of an implicit assumption that we can ignore the signal degradation due to the additional loss caused by the cord. The assumption is reasonable and justified because the cord length is less than a few hundred meters.

When an H-OTDR is designed as shown in **Fig. 6**, the single-way dynamic range (SWDR) of the H-OTDR is given by[20]

$$SWDR_{isolation} = \frac{P_{peak0} - P_{APD} - R_{SWPF} - L_{AO} + SNIR/2}{2} \text{ (in dB)} \quad (14)$$

where P_{peak0} is the output peak power from the H-OTDR light source, P_{APD} is the minimum detectable power of the H-OTDR receiver, R_{SWPF} is the return loss of an SWPF at the measurement wavelength, L_{AO} is the roundtrip loss of an acousto optic (AO) switch used as a directional coupler, and SNIR is the signal-to-noise ratio (SNR) improvement as a result of averaging over a number of reflected pulses. Here an AO switch is used in the H-OTDR because the roundtrip loss of an AO switch is usually less than that of a conventional

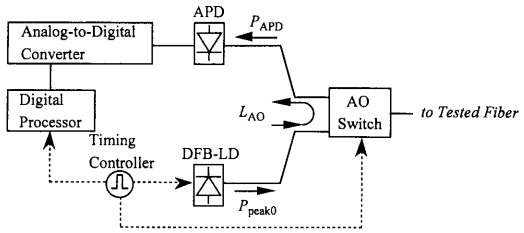

Fig.6 Configuration of high spatial-resolution OTDR (H-OTDR).

3-dB optical coupler. To enhance the dynamic range of the H-OTDR, an avalanche photodiode (APD) is employed as the H-OTDR receiver.

For this case, the minimum detectable power P_{APD} which is defined as the power giving SNR = 1 satisfies the following relation:

$$\langle I\rangle^2 = \sigma^2_{shot} + \sigma^2_{thermal} \tag{15}$$

with

$$\langle I\rangle = M_A(P_{APD}\, e\rho/h\nu) \tag{16}$$

$$\sigma^2_{shot} = 2e(P_{APD}\, e\rho/h\nu + i_d)B_{OTDR}M_A^2F(M_A) \tag{17}$$

and

$$\sigma^2_{thermal} = 4k_BTB_{OTDR}/R_L \tag{18}$$

where $\langle I\rangle$ is the average photocurrent at the APD, σ^2_{shot} is the variance of the shot noise current, $\sigma^2_{thermal}$ is the thermal noise variance at the APD, M_A is the multiplication factor of the APD, e is the electronic charge, ρ is the photodiode quantum efficiency, h is Plank's constant, ν is the frequency of light, i_d is the dark current of the APD, B_{OTDR} is the H-OTDR receiver bandwidth, $F(M_A)$ is the excess noise factor of the APD, k_B is Boltzmann's constant, T is the absolute temperature, and R_L is the receiver load resistance which is related to the junction capacitance C_d as

$$R_L = \frac{1}{2\pi C_d B_{OTDR}}. \tag{19}$$

The excess noise factor $F(M_A)$ increases with the factor M_A and is given by

$$F(M_A) = k_AM_A + (1-k_A)\cdot(2-1/M_A) \tag{20}$$

where k_A is the ionization coefficient ratio for the excess noise of the APD, which is in the range of 0 to 1 depending on the semiconductor material used to make up the APD.

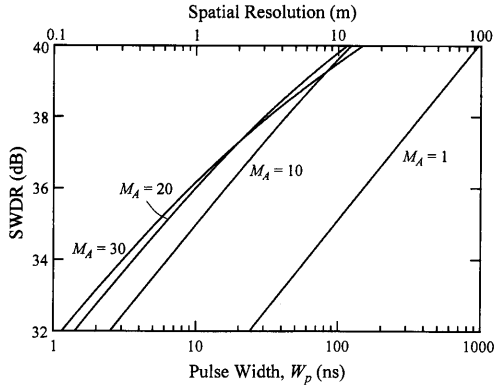

Fig.7 Single-way dynamic range (SWDR) of an OTDR as a function of the pulse width for several multiplication factors. In this calculation, the peak power is 13dBm, the return loss of the SWPF is 20dB, and the 2^{16} reflected pulses are averaged. The spatial resolution is calculated from Eq. (1) with νgr = $2.0 \cdot 10^8$m/s.

When the pulse width W_p of the H-OTDR light is assumed to be the inverse of B_{OTDR}, the SWDR is related to W_p from Eqs. (14) to (20). The calculated result is shown in **Fig.7** for several multiplication factors M_A, where we assume that P_{peak0} = 13dBm, L_{AO} = 4dB, and SNIR = 48dB for averaging over 2^{16} reflected pulses. In the calculation, APD's parameters were assumed that ρ = 0.85, k_A= 0.7, i_d = 2nA, C_d = 1pF and T = 298K. In **Fig. 7**, the APD is more effective than a *pin* receiver (M_A = 1) in increasing the dynamic range. When $M_A > 20$, however, the effect of the avalanche multiplicative gain decreases because of an increase in the excess noise given by Eq. (17). It is interesting to note that the SWDR decreases as the OTDR pulse width is reduced, since the minimum detectable power at the APD increases with a reduction in W_p.

3.3 Targets for Key Devices

Table 1 shows our target for an SWPF designed to isolate faults in an optical PDS network. The transmission losses for the signal and measurement wavelengths must be less than 1dB and more than 34dB, respectively. Specifically, the required transmission loss for the measurement wavelength was estimated from **Fig.2** when we assumed that the tolerance of the CNR decrease was 0.2dB and the peak power of 10-ns H-OTDR pulses was 0dBm at the SWPF input port. In contrast, the return losses for the signal and measurement wavelengths should be more than 35dB

Table 1 Targets for key devices for fault location during in-service testing in optical PDS networks.

Device	Item	Target
SWPF	Transmission Loss	≤ 1 dB (at 1.3/1.55-μm wavelengths) ≥ 34 dB (in 1.6-μm band)
	Return Loss	≥ 35 dB (at 1.55-μm wavelength) ≤ 20 dB (in 1.6-μm band)
H-OTDR	Resolution	≤ 1 m
	SWDR	≥ 36 dB

and less than 20dB, respectively. Ideally, we should aim for a return loss of less than 14dB in the 1.6-μm band, because the return loss of Fresnel reflection with a perfect fiber end is 14dB. If the ideal loss is achieved in an SWPF, we can always isolate any fault even if the fault is the result of a fiber break with perfect Fresnel reflection just in front of an ONU. However, as shown in **Fig.4**, it is difficult to realize both a 14-dB return loss in the 1.6-μm band and a 35-dB return loss for the 1.55-μm wavelength in an SWPF with the configuration shown in **Fig.3**. We therefore set our target for the return loss in the 1.6-μm band at less than 20dB, which is the best performance achievable with the configuration of **Fig.3**, to enable the faults to be isolated as easily as possible.

Table 1 also shows our target for the spatial resolution and dynamic range of an H-OTDR. The required spatial resolution is specified to be less than 1 m to reduce the CSO degradation due to additional cords to 0.2dB as shown in **Fig. 5**. To determine our target for the SWDR of the H-OTDR, the transmission line loss in the 1.6-μm band must be estimated. According to sample measurements made in optical access networks in metropolitan Japan[21], the 7-km transmission line loss in the 1.6-μm band is 12.8dB with a 99 % probability. From the result, the transmission line loss is estimated to be less than 26 (=12.8+12+1.2) dB in an optical PDS network with a 16-branch optical splitter including the excess loss of 1.2dB. Since the combined coupling loss of a fiber selector and a WINC is 10dB, the SWDR of the H-OTDR must be more than 36dB.

4. Characteristics for Fabricated SWPF and H-OTDR

4.1 1.6-μm Band SWPF Embedded in SC-Connector

Table 2 shows the characteristics of fabricated SWPFs in which an optical interference filter was embedded in an SC connector with an inclination angle of 3.5 degrees. We fabricated the filter by depositing multilayers of TiO_2 and SiO_2 on a polyimide film substrate, and its thickness was about 30 μm[18]. The transmission losses for both the 1.31-μm and 1.55-μm wavelengths were less than 0.9dB. The return losses for the 1.55-μm and 1.65-μm wavelengths were more than 38dB and approximately 20dB, respectively. The transmission loss for the 1.65-μm wavelength was more than 34dB.

Table 2 Characteristics of fabricated SWPFs.

Wavelength	1.31/1.55 μm (Signal)	1.65 μm (Measurement)
Transmission Loss	< 0.9 dB	> 34 dB
Return Loss	> 38 dB	~ 20 dB

4.2 1.6-μm Band H-OTDR

An H-OTDR system as shown in **Fig.6** was constructed by using the design technique developed in Sec. 3. H-OTDR pulses are generated by directly modulating the distributed feedback laser diode (DFB-LD) with a center wavelength of 1.654 μm, and they are emitted via an AO switch. Since we could easily obtain a DFB-LD whose temporal response was high enough to form narrow pulses, we adopted it as the H-OTDR light source. The optical peak power from the laser was about 13 dBm. **Figure 8** shows the pulse waveform at the output port of the H-OTDR, and the full width at half maximum (FWHM) was 9.6 ns. The back-reflected pulses are received at an APD via the AO switch with a roundtrip loss of 4dB. The APD's parameters were identical to those used in the Sec. 3 at a multiplication factor M_A of 20. The bandwidth of the H-OTDR receiver was 100MHz as shown in **Fig. 9**.

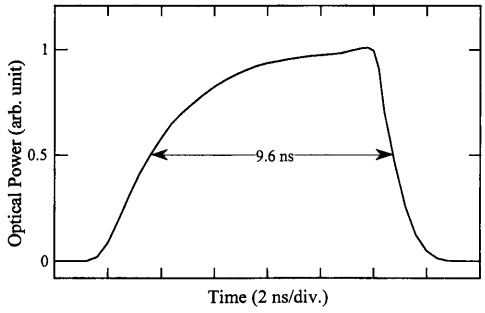

Fig.8 Pulse waveform of the H-OTDR used in the experiment. The pulse width (FWHM) is 9.6 ns.

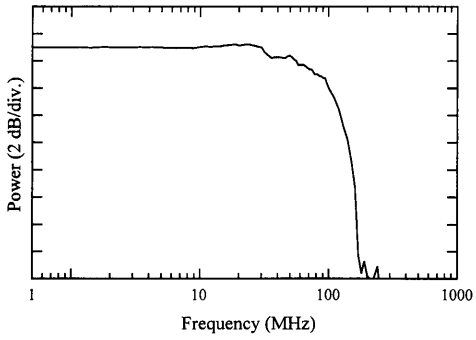

Fig.9 Frequency characteristics of the H-OTDR receiver. The bandwidth is 100MHz.

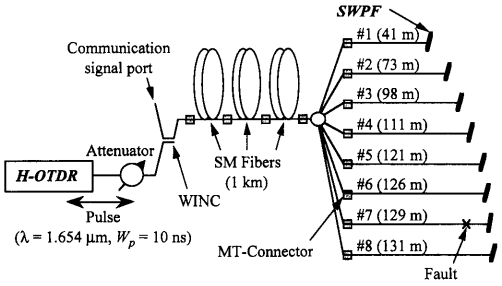

Fig.10 Experimental setup for isolating a fault in an optical PDS network. The number in round brackets denotes the branched fiber length.

To confirm the performance of the H-OTDR, we carried out fault isolation experiments in the setup shown in **Fig.10**. The transmission line is composed of a non-branched common optical fiber, an eight-branch optical splitter and eight branched optical fibers. The 3-km long non-branched common optical fiber consists of three 1-km long single-mode (SM) fibers that are joined with mechanically transferable (MT) connectors. The lengths of the branched fibers are 41, 73, 98, 111, 121, 126, 129 and 131m, respectively. The loss of each line was about 13dB including the splitting loss of the splitter. An SWPF with a return loss of 20dB at the 1.65-μm wavelength is placed at the far end of each branched fiber. A WINC with a coupling loss of about 8dB is positioned between the H-OTDR and the transmission line. An optical attenuator is installed in front of the H-OTDR to estimate its dynamic range.

The H-OTDR trace reflected from eight SWPFs is shown in **Fig.11** when the attenuation of the optical attenuator was 7dB and the 2^{16} pulses were averaged. Although all the reflected signals are superimposed in one H-OTDR trace and the difference between the lengths of the seventh and eighth branched optical fibers is only 2 m, all the

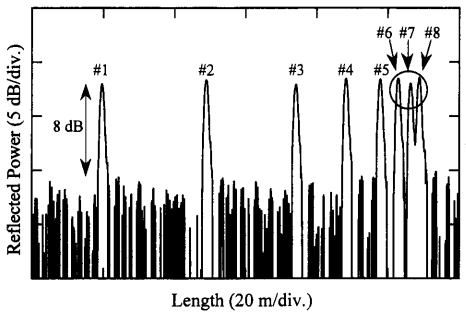

Fig.11 H-OTDR trace showing the reflected power distribution in the fault isolation experiment when the number of averaged pulses and return loss of the SWPF for the 1.65-μm wavelength are 2^{16} and 20dB, respectively.

reflection peaks from the SWPFs can be distinguished in the trace. From the figure, the single-way dynamic range of the H-OTDR is 36dB when we consider the following two points. First, the power ratio of the reflected light from the SWPF to the equivalent noise of the OTDR is 8dB, which is directly observed from the trace. Second, the total line loss from the OTDR is 28 (=7+8+13) dB. As we expected, the experimental result for the SWDR agrees with the theoretical prediction shown in **Fig.7. Figures 12(a) and (b)** show H-OTDR traces without and with a fiber fault in seventh branched fiber, respectively[22]. The fault was generated by bending the seventh fiber with a resultant loss of 3dB. These figures are enlargements of the area indicated by the circle in **Fig.11**. Only the peak of the seventh fiber in the H-OTDR trace (b) is 3dB lower than its initial value shown in (a). The noticeable feature is that the spatial resolution of the H-OTDR is 1 m since the full width at 1.5-dB maximum is confirmed as 1 m for the observed light from one SWPF in the trace.

5. Fault Isolation Experiments in a Field Trial

To clarify the feasibility of fiber-to-the-home (FTTH), a field trial has been carried out in Kansai-Science-City in Japan[23]. In the trial, multimedia services such as ISDN and video distribution have been provided using the optical PDS networks shown in **Fig.1.** An H-OTDR, which satisfies all the requirements listed in **Table 1**, has been operated to isolate faults in the working PDS networks. **Figure 13** shows an example of the H-OTDR trace observed for an optical line with seven SWPFs. There are seven customers, and the lengths of the branched optical fibers are

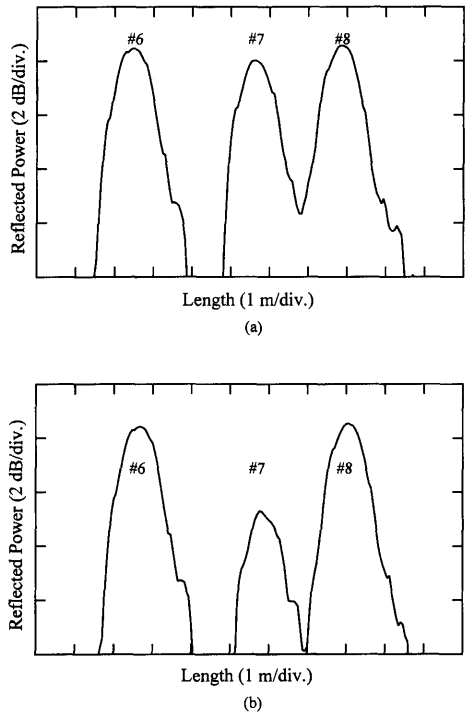

Fig.12 H-OTDR traces: (a) without a fiber fault, (b) with a fiber fault. In the experiment, the fault was generated by bending the seventh fiber with a resultant loss of 3dB.

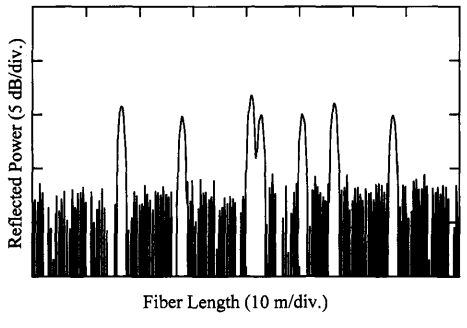

Fig.13 Experimentally observed H-OTDR trace in a field trial in Kansai-Science-City.

24, 36, 49, 51, 58, 64 and 75m, respectively. We can see that individual customers are clearly distinguished in the designed H-OTDR trace. It is also confirmed that the ISDN and video signal quality has not degraded when the SWPFs described in the preceding section are used in the working PDS networks.

6. Conclusion

This paper described a practical fault-isolating technique and system design for using in a working passive double star (PDS) networks with outside splitters. The system has two features. The first involves installing a short wavelength pass filter (SWPF) that is embedded in a single-fiber-coupling (SC) connector. We designed the SWPF to prevent the light of an optical time domain reflectometer (OTDR) operating in the 1.6-μm band from entering an optical network unit (ONU) and to obtain back-reflected light power that is sufficiently high to provide the dynamic range of an OTDR. In actual, we obtained the SWPF with a transmission loss of 34dB and a return loss of 20dB for a wavelength of 1.65 μm. The SWPF was also designed that the return loss for the signal wavelength was more than 35dB, because the signal quality is very sensitive to multiple reflections in optical transmission lines.

The second feature is the enhancement of the spatial resolution of the OTDR to 1 m at the operating wavelength of 1.65 μm. This OTDR was called H-OTDR in this paper. The high spatial-resolution was obtained by narrowing the H-OTDR pulse width and widening the receiver bandwidth of the H-OTDR. Although the difference between the lengths of branched optical fibers was only 2 m, the reflection from each SWPF could be isolated in one H-OTDR trace. To allow us to incorporate the H-OTDR in working optical PDS networks, the H-OTDR was also designed so that its single-way dynamic range would be more than 36dB when averaging the back-reflected 2^{16} pulses with the return loss of 20dB.

The designed fault-isolating system has been employed in a field experiment on new multimedia info-communication services with wavelength division multiplexing (WDM) techniques in Kansai-Science-City. The results of measurement confirmed that the proposed system is effective for isolating faults in optical PDS networks despite the test fibers being in service.

Acknowledgment

The authors would like to thank Dr. T. Horiguchi of NTT Access Network Service Systems Laboratories, Dr. S. Furukawa of Yazaki Corporation, and Prof. Y. Koyamada of Ibaraki University for their valuable comments and discussions.

References

1) W. I. Way, "Subcarrier multiplexing lightwave system design considerations for subscriber loop applications," *IEEE J. Lightwave Technol.* vol. 7, no. 11, pp. 1806-1818, 1989.

2) K. Okada and F. Mano, "Passive double star system features," in *Proc. 3rd IEEE Workshop Local Optical Net-*

works, paper 5.1, 1991.

3) N. J. Frigo, "Local access optical networks," *IEEE Network*, vol. 5, no. 6, pp. 32-36, 1996.

4) I. Yamashita, T. Kanada, and K. Harikae, "PDS Technologies realizing economical full access network operation," *NTT Review*, vol. 9, no. 5, pp. 38-43, 1997.

5) ITU-T. *Recommendation* G.983.1, "Broadband optical access systems based on passive optical networks (PON)," 1998.

6) R. D. Feldman, T. H. Wood, J. P. Meester, and R. F. Austin, "Broadband upgrade of an operating narrowband single-fiber passive optical network using coarse wavelength division multiplexing and subcarrier multiple access," *IEEE J. Lightwave Technol.* vol. 16, no. 1, pp. 1-8, 1998.

7) P. P. Iannone, N. J. Frigo, and K. C. Reichmann, "A repeated regional/WDM local access network for delivery of broadcast digital TV," in *Proc. OFC '99*, pp. 324-326, 1999.

8) T. H. Wood, G. C. Wilson, R. D. Feldman, and J. A. Stiles, "Fiber vista: A cost-effective fiber-to-the-home (FTTH) system providing broad-band data over cable modems along with analog and digital video," *IEEE Photon. Tecnol. Lett.*, vol. 11, no. 4, pp. 475-477, 1999.

9) H. Takasugi, N. Tomita, T. Uenoya, I. Nakamura, and Y. Yokoo, "Design and evaluation of automatic optical fiber operation support systems," in *Proc. Int. Wire Cable Symp.*, pp. 623-629, 1990.

10) Y. Koyamada, N. Ohta, and N. Tomita, "Basic concepts of fiber optic subscriber loop operation systems, "in *Proc. Int. Conf. Commun.*, pp. 1540-1544, 1990.

11) N. Tomita, H. Takasugi, N. Atobe, I. Nakamura, F. Takaesu, S. Takashima, "Design and performance of a novel automatic fiber line testing system with OTDR for optical subscriber loops," *IEEE J. Lightwave Technol.* vol. 12, no. 5, pp. 717-725, 1994.

12) H. Iwata, S. Tomita, M. Matsumoto, and T. Tanifuji, "Bragg reflection optical memory for passive branched optical network management," in *Proc. Int. Workshop on Optical Access Networks*, pp. 6.3.1-6.3.9, 1994.

13) H. Ogura, T. Toide, H. Miyazaki, S. Sugimoto, and A. Sonoda, "Launch of 'CATV video distribution service' over FTTH," *NTT Review*, vol. 9, no. 6, pp. 104-112, 1997.

14) F. Yamamoto, and T. Horiguchi, "Allowable received OTDR light power for in-service measurement in lightwave SCM systems," *IEEE J. Lightwave Technol.*, vol. 18, no. 3, pp. 286-294, 2000.

15) M. Saruwatari, and K. Nawata, "Semiconductor laser to single-mode fiber coupler," *Appl. Opt.*, vol. 18, no, 11, pp. 1847-1856, 1979.

16) H. Yoshinaga, K. Kikushima, and E. Yoneda, "Influence of reflected light on Erbium-doped fiber amplifiers for optical AM video signal transmission systems," *IEEE J. Lightwave Technol.*, vol. 10, no. 8, pp. 1132-1136, 1992.

17) S. Nagasawa, H. Furukawa, M. Makita, and H. Murata, "Mechanically transferable single-mode multifiber connectors," *IOOC '89 Tech. Digest*, p. 21C2-1, 1989.

18) T. Oguchi, J. Noda, H. Hanafusa, and S. Nishi, "Dielectric Multilayered interference filters deposited on Polyimide films," *Electron. Lett.*, vol. 27, no. 9, pp.706-707, 1991.

19) C. Y. Kuo and E. E. Bergmann, "Low distortion amplified analog CATV transport system," in *Proc. OFC '92*, pp. 336-338, 1992.

20) F. Yamamoto, S. Furukawa, H. Suda, and Y. Koyamada, "Fault isolation technique using high resolution 1.6-μm band OTDR for passive double star networks," in *Proc. 6th Int. Workshop on Optical Access Networks*, pp. 6.2.1-6.2.7, 1994.

21) F. Yamamoto, S. Furukawa, H. Suda, and Y. Koyamada, "Measurement using 1.6-μm band wavelength in optical subscriber networks," in *Proc. IEICE '94 Spring Conf.*, p. B-981, 1994.

22) F. Yamamoto, S. Furukawa, H. Suda, and Y. Koyamada, "1.6-μm band fault isolation technique for passive double star networks," in *Proc. IEICE '94 Fall Conf.*, p. B-846, 1994.

23) S. Furukawa, H. Suda, F. Yamamoto, Y. Koyamada, T. Kokubun, and I. Takahashi, "Optical fiber line test and management system for passive double star networks and WDM transmission systems," in *Proc. Int. Wire Cable Symp.*, pp. 640-648, 1995.